Magnetic Diagnostics of Magnetic Island in LHD

Y. NARUSHIMA, K.Y. WATANABE, S. SAKAKIBARA, N. OHYABU, H. YAMADA, K. NARIHARA, I. YAMADA, T. MORISAKI, S. INAGAKI, Y. NAGAYAMA, A. KOMORI, LHD exp. group and W.A. COOPER[1)]

National Institute for Fusion Science, Toki, Gifu 509-5292, Japan
[1)]*CRPP Association Euratom/Confederartion Suisse, EPFL, 1015 Lausanne, Switzerland*

(Received 13 December 2006 / Accepted 23 April 2007)

Characteristics of magnetic islands are investigated by magnetic diagnostics in the Large Helical Device (LHD). The structure of the magnetic island with $m/n = 1/1$ (where, m and n are poloidal and toroidal mode number, respectively) can be estimated from the perturbed magnetic field appearing when a magnetic island changes. To measure the toroidal profile of the perturbed magnetic field δb_1 originating from the plasma, a toroidal array of magnetic flux loops is set up in the LHD. The toroidal profile of δb_1 is then spatially Fourier decomposed to determine the amplitude of the $n = 1$ component, $\delta b_1^{n=1}$ and its phase, $\phi_{n=1}$ which correspond the change of the island width and the toroidal position of the X-point of the island, respectively. Therefore, the information about the magnetic island structure can be obtained from $\delta b_1^{n=1}$ and $\phi_{n=1}$. In case the island width becomes larger than the seed island, measurements show that $\delta b_1^{n=1}$ is non-zero and $\phi_{n=1}$ is temporally constant. A non-zero $\delta b_1^{n=1}$ can also be observed when the island width becomes smaller than the seed island. In this case, the angle $\phi_{n=1}$ shifts by about π[rad] compared with the increasing case and the $\delta b_1^{n=1}$ is limited to a certain value which corresponding to the magnetic field suppressing the seed island.

Keywords: Large Helical Device, magnetic island, magnetic diagnostics, self-healing

DOI: 10.1585/pfr.2.S1094

1. Inroduction

Magnetic islands sometimes play key roles in the toroidal plasma confinement from the viewpoint of Magneto-Hydro Dynamic (MHD) stability. In tokamaks, for example, a seed island triggers a neoclassical tearing mode (NTM), and its growth leads to a serious deterioration of plasma confinement [1,2]. Some studies about magnetic islands have been investigated in the Large Helical Device (LHD) [3–5]. It has been reported that the magnetic island width enlarges or shrinks depending on some plasma parameters. Especially, the magnetic island disappears at lower collisionality and higher beta. In the above studies in the LHD, the width of the local flattening shape of the electron temperature (T_e) profile measured by the Thomson scattering [6] is used as a rough guide of the magnetic island. This is because it is thought that the isotemperature surface reflects the magnetic surface structure very well due to the faster velocity of the parallel movement than that of the perpendicular diffusion. The Thomson scattering system with high spatial resolution (137 points on the major radial direction) has been a powerful tool to study the magnetic island in the LHD. However, the profile can be obtained at only one toroidal position $\phi = 108$ [deg] along the equatorial plane as shown in Fig. 1. Therefore, the analysis combined with the other measurement techniques is required for a more detailed investigation of the magnetic island.

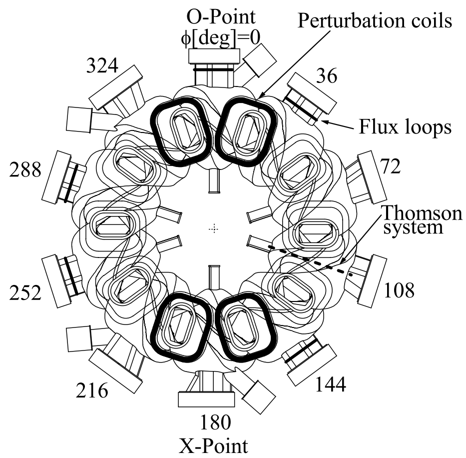

Fig. 1 Top view of the vacuum vessel of LHD. Toroidal angle ϕ is defined as a positive with clockwise.

It is known that a magnetic island is formed when a perturbed magnetic field resonates at a rational surface fixed by the magnetic configuration. In a toroidal magnetic confinement device with major radius R and toroidal magnetic field B_t, the amplitude of the perturbed magnetic field δb with a certain Fourier component having poloidal mode number m resonates at a rational surface with a rotational transform ι at minor radius r. The resultant magnetic

author's e-mail: narusima@LHD.nifs.ac.jp

island width w can be determined as follows [7]:

$$w^2 = 2\pi(16R/m)(d\iota/dr)^{-1}(\delta b/B_t). \quad (1)$$

It should be noted that the w is proportional to the square root of δb. In this study, δb can be categorized into two kinds of magnetic field. One is a static magnetic field δb_0 that is constant during the plasma discharge, which is generated by the perturbation coils and produces the static seed island described in section 2. Another kind of the magnetic field is a time-varying magnetic field δb_{pl} which appears when the magnetic island width changes during the plasma discharge. Because the δb_{pl} provides useful data about the structure of the island, measurement of δb_{pl} is an effective method to research magnetic islands.

This paper is organized as follows. The experimental setup is described in the following section. In section 3, the analysis method of the magnetic diagnostics is explained. The experimental results are shown in section 4. We will discuss the results in section 5 and finally, summarize in section 6.

2. Experimental Set-up

2.1 Perturbation coil system to produce seed island

The 4-pairs of perturbation-coils placed at the top and bottom of the LHD at around the toroidal angle of $\phi = 0$ and 180 [deg] (denoted by bold solid line in Fig. 1) produce a resonant field δb_0 having a spatial perturbation of $m/n = 1/1$ mode [8] (here, n is the toroidal mode number). The δb_0 resonates with the confinement magnetic field on the $\iota/2\pi = 1$ rational surface to produce the seed island with $m/n = 1/1$ mode, whose X (O)-point stays at the outer board side at $\phi = 180$ (0) [deg]. This seed island itself does not rotate and its width is constant because the perturbation-coil current is temporally constant during a discharge. Changing the perturbation-coil current in different discharges can vary the seed island width via the change of δb_0.

2.2 Measurement of the magnetic island by magnetic diagnostics

To estimate the δb_{pl}, we measure the perturbed magnetic field using a toroidal array of 5 magnetic flux loops set at the outer ports in the LHD as shown in Fig. 1 [9]. Each flux loop has $N = 10$ [turn] wound at the ports whose cross-sections are $S = 1.2\,[\mathrm{m}^2]$ and have a total cross-section of $NS = 12\,[\mathrm{m}^2\mathrm{turn}]$, which detects the component of the magnetic field in the major radial direction. During a plasma discharge, these loops can detect only the perturbed magnetic flux Φ^R originating from δb_{pl} since δb_0 is temporally constant during the discharge. As a result, the δb_1 that is proportional to δb_{pl} can be obtained from the average value of the major radial component of the perturbed magnetic field at the flux loop ($\delta b_1 = \Phi^R/NS$).

3. Analysis Methods of Magnetic Diagnostics

As we have described, the magnetic island width can be estimated by measuring δb_0 and δb_{pl}. The δb_0 can be obtained from the calculation with the Biot-Savart law using the current flowing in the perturbation coils, which decides a seed magnetic island width w_{seed}. On the other hand, δb_{pl} can be estimated from the δb_1. Therefore, detailed diagnostics of δb_1 is required. As shown in Eq. (1), the magnetic island width is proportional to the square root of the δb which is comprised of both δb_0 and δb_{pl} [4]:

$$w^2 = 2\pi(16R/m)(d\iota/dr)^{-1}\{(\delta b_0 + \delta b_{pl})/B_t\}. \quad (2)$$

In case of the $\delta b_0 = 0$ and non-zero δb_{pl}, the island width is defined as w_{pl}.

$$w_{pl}^2 = 2\pi(16R/m)(d\iota/dr)^{-1}(\delta b_{pl}/B_t) \quad (3)$$

The w_{pl} can be estimated by the amplitude with the $n = 1$ component ($\delta b_1^{n=1}$) of the toroidal profile of the δb_1 because the δb_{pl} is proportional to the $\delta b_1^{n=1}$ and the magnetic island studied here has the $m/n = 1/1$ mode structure.

$$w_{pl}^2 = \alpha(\delta b_1^{n=1}/B_t) \quad (4)$$

The coefficient α makes the connection between the w_{pl} and the $\delta b_1^{n=1}/B_t$. It is thought that the coefficient α is constant under the condition in which the magnetic configuration (magnetic shear, position of the resonant surface) does not change. The α can be obtained from the calculation with the Biot-Savart law assuming the multi-filament current on the resonant surface of $\iota/2\pi = 1$. The Poincaré plot of the magnetic island produced by the filament currents is shown in Fig. 2 (a) at the toroidal angle ($\phi = 108$ [deg]) where the T_e profile is measured. The

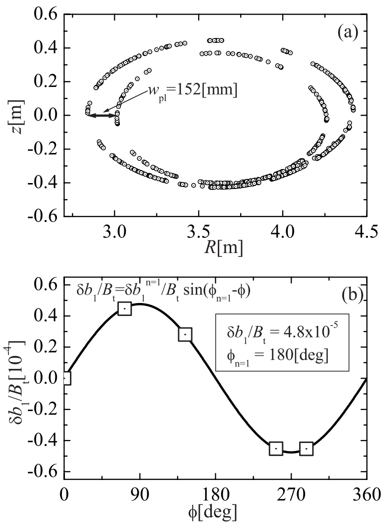

Fig. 2 (a) Poincaré plot of magnetic island produced by the filament currents. (b) Toroidal profile of the pertubed magnetic field.

toroidal profile of the δb_1 is shown by the open squares in Fig. 2 (b). In the vacuum configuration, the δb_0 makes the seed island with width of $w_{\rm seed}$. From the $w_{\rm seed}$ and Eq. (4), the magnetic island width $w_{\rm mag}$ derived from the magnetic diagnostics is presented as follows.

$$w_{\rm mag}^2 = \alpha(\delta b_1^{n=1}/B_{\rm t}) + w_{\rm seed}^2 \tag{5}$$

Here, we define the $\delta b_1^{n=1}/B_{\rm t}$ to be negative when the magnetic island shrinks ($w < w_{\rm seed}$). The amplitude of the $n=1$ component $\delta b_1^{n=1}$ is an important value to estimate the width of the magnetic island $w_{\rm mag}$ with the magnetic diagnostics (Eq. (5)). The toroidal profile of the δb_1 is decomposed to the $n=1$ mode with the Fourier decomposition to define the $\delta b_1^{n=1}$ and $\phi_{n=1}$ which is the toroidal position of the X-point of the island at outboard side of the torus. As the result, the spatially Fourier decomposition of the $n=1$ component of the toroidal profile of $\delta b_1(\phi)$ can be obtained from the signals of the 5 flux loops from the following equations.

$$\delta b_1(\phi) = \delta b_1^{n=1}\sin(\phi_{n=1} - \phi) \tag{6}$$

The $\delta b_1^{n=1}$ and $\phi_{n=1}$ are represented as follows.

$$\delta b_1^{n=1} = \sqrt{B_{\rm s}^2 + B_{\rm c}^2} \tag{7}$$

$$\phi_{n=1} = \arctan(B_{\rm s}/B_{\rm c}) + \pi/2 \tag{8}$$

here, the $B_{\rm s}$ and $B_{\rm c}$ are obtained by the measured perturbed field δb_1^i at each toroidal position $\phi_{\rm i}$.

$$\begin{aligned} B_{\rm s} &= \sum_{i=1}^{5}\delta b_1^i \sin(n\phi_i)\Bigg/\sum_{i=1}^{5}\{\sin(n\phi_i)\}^2 \\ B_{\rm c} &= \sum_{i=1}^{5}\delta b_1^i \cos(n\phi_i)\Bigg/\sum_{i=1}^{5}\{\cos(n\phi_i)\}^2 \end{aligned} \tag{9}$$

4. Magnetic Island During Plasma Discharge

The typical discharge with a seed island ($w_{\rm seed} = 160$ [mm]) is shown in Fig. 3. The time evolution of the $w_{\rm TS}$ which is the width of the flattening region of the $T_{\rm e}$ profile at inboard side of the major radius shows the increasing trend from 160 to 200 [mm] as shown in Fig. 3 (d). The scattering of the data is originated from the measurement error of the Thomson system. The time evolution of the $\delta b_1^{n=1}/B_{\rm t}$ and $\phi_{n=1}$ are shown in Fig. 3 (e) (f). The $\delta b_1^{n=1}/B_{\rm t}$ increases from $\delta b_1^{n=1}/B_{\rm t} = 0$ to 0.5×10^{-4} and the $\phi_{n=1}$ does not change ($\phi_{n=1} \sim 180$ [deg]) during the plasma discharge. These results mean that the magnetic island width increases during plasma discharge without rotation.

The radial profile of $T_{\rm e}$ and the toroidal profile of $\delta b_1/B_{\rm t}$ at $t = 0.48$ and 1.73 [s] are shown in Fig. 4. At $t = 0.48$ [s] (Fig. 4 (a)), the $T_{\rm e}$ profile shows the local flattening region with the width almost same as the $w_{\rm seed}$. At the same time, the flux loops do not detect the $\delta b_1/B_{\rm t}$ as

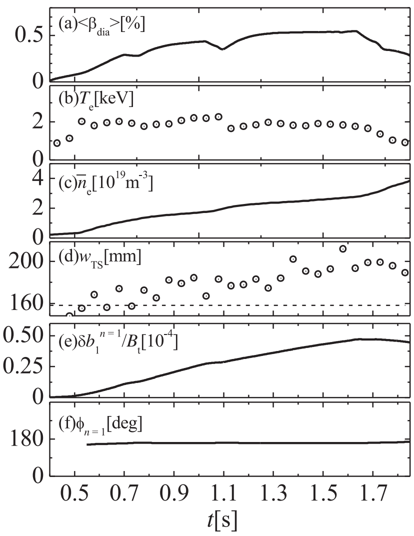

Fig. 3 Time evolution of (a) averaged beta $< \beta >_{\rm dia}$ (b) electron temperature $T_{\rm e}$ (c) averaged electron density $n_{\rm e}$ (d) island width $w_{\rm TS}$ (e) amplitude of $n = 1$ mode δb_1 (f) toroidal angle $\phi_{n=1}$

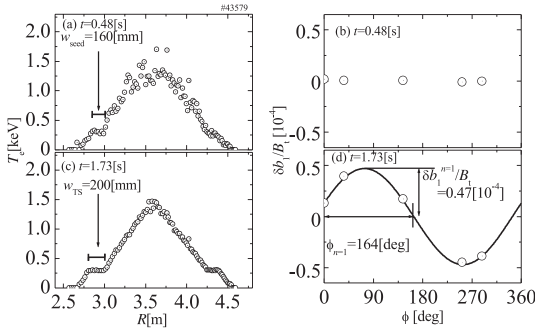

Fig. 4 $T_{\rm e}$ and $b_1^{n=1}/B_{\rm t}$ profile at (a) (b) $t = 0.48$ [s], (c) (d) 1.73 [s].

shown in Fig. 4 (b), which means that the magnetic island does not change. In other words, the magnetic island maintains its shape of the seed island. At $t = 1.73$ [s], the island width becomes $w_{\rm TS} = 200$ [mm] (Fig. 4 (c)) and the finite perturbed magnetic field $\delta b_1/B_{\rm t}$ appears as shown in Fig. 4 (d). In this time, the $\delta b_1^{n=1}/B_{\rm t}$ and the $\phi_{n=1}$ are 0.5×10^{-4} and 164 [deg], respectively. The estimated width of the magnetic island is $w_{\rm mag} = 219$ [mm] which is 10 % different from the $w_{\rm TS} = 200$ [mm]. The relationship between the $w_{\rm TS}^2$ and the $\delta b_1^{n=1}/B_{\rm t}$ is shown in Fig. 5 in a discharge with the $w_{\rm seed} = 116$ [mm]. The solid line shows the theoretical value obtained from the Eq. (5). The scattering of the data is originated from the measurement error of the Thomson system and might be brought by the deviation of the $T_{\rm e}$ profile from the magnetic surface structure by the effect of perpendicular diffusion of the electron. The spatial resolution of the Thomson system is about 20 mm, which restricts the spatially precise measurement of the $w_{\rm TS}$ in a small level. Therefore, it is difficult to estimate

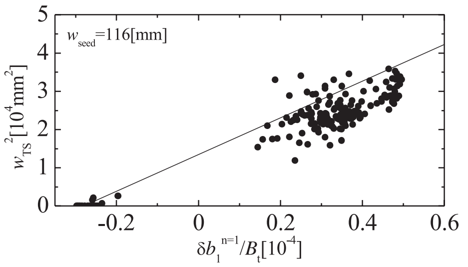

Fig. 5 Relationship between w^2_{TS} and $b^{n=1}_1/B_t$.

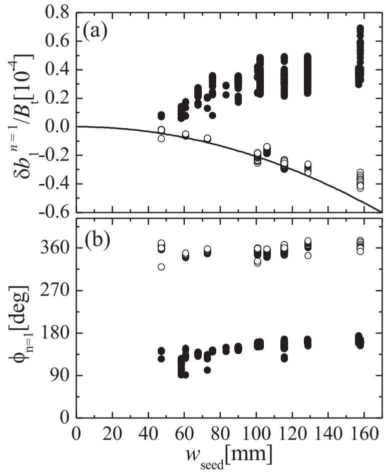

Fig. 6 The w_{seed} dependency of (a) $b^{n=1}_1/B_t$ and (b) $\phi_{n=1}$. The solid line in (a) denotes the corresponding magnetic field strength required to suppress the seed magnetic island.

the magnetic island width with the Thomson scattering correctly.

Figure 6 shows the w_{seed} dependency of the $\delta b^{n=1}_1/B_t$ and $\phi_{n=1}$. In Fig. 6 (a), the filled circle means that the magnetic island width enlarges. The open circle means that the w_{TS} cannot be determined, that is, $w_{TS} = 0$ (self-healing [3]). When the magnetic island width enlarges, the $\delta b^{n=1}_1/B_t$ increases with w_{seed} and the $\phi_{n=1}$ is distributed over the range $\phi = 90$ to 180 [deg]. In the case of $w_{TS} = 0$, the absolute value of the $\delta b^{n=1}_1/B_t$ increases with w_{seed}. The solid line shows the $\delta b_1/B_t$ obtained from Eq. (3) with $w_{mag} = 0$, which is corresponding to the envelope of the experimental data. The angle $\phi_{n=1}$ shifts by 110 [deg] or more as contrasted with the increasing case. The T_e and $\delta b_1/B_t$ profile in case of the finite $\delta b_1/B_t$ and $w_{TS} = 0$ is shown in Fig. 7. The angle $\phi_{n=1}$ shifts by 190 [deg] from the increasing case shown in Fig. 4 (d). The amplitude of the perturbed magnetic field is $\delta b^{n=1}_1/B_t = -0.26 \times 10^{-4}$ in which the w_{pl} is estimated as $w_{pl} = -112$ [mm] from Eq. (2), whose absolute value corresponds to the width of the seed island $w_{seed} = 114$ [mm].

5. Discussion

The time evolution of the w_{TS} shows an increasing trend from 160 to 200 [mm] as shown in Fig. 3,(d).

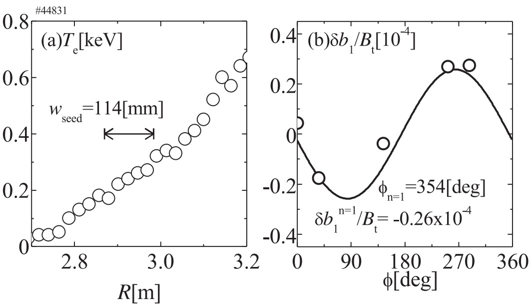

Fig. 7 (a) T_e and (b) $b^{n=1}_1/B_t$ profile in case the magnetic island disappears. The seed island width is $w_{seed} = 114$ [mm].

This means that the magnetic island width enlarges at $\phi = 108$ [deg]. Whether this phenomenon shows the growth or the rotation of the magnetic island cannot be distinguished because the Thomson scattering measures the T_e profile at only $\phi = 108$ [deg]. For example, when the magnetic island rotates without growth of the width, or the width of the magnetic island increases without rotation, it seems that w_{TS} changes in appearance. On the other hand, the magnetic diagnostics bring the detailed information of the dynamics and the structure of the magnetic island.

When the magnetic island width with the $m/n = 1/1$ mode becomes larger than w_{seed} during a discharge, the toroidal profile of the $\delta b_1/B_t$ shows the $n = 1$ mode structure with constant $\phi_{n=1}$ which is same as that of the seed island. This phenomenon means that a certain current with $m/n = 1/1$ structure flows in the plasma to enlarge the magnetic island without the rotation. According to the theoretical study [10], the Pfirsch-Schluter current modified by the magnetic island enlarges the magnetic island in Heliotron plasma, which might be a clue to find the mechanism to drive that current. Further analyses are required to distinguish the kind of the current.

The finite $\delta b_1/B_t$ is also observed when the island width disappears. In this time, the polarity of the perturbed magnetic field is opposite to the increasing case. The $|\delta b^{n=1}_1/B_t|$ does not exceed a certain value of $\delta b^{n=1}_1/B_t = -w^2_{seed}/\alpha$ which corresponds to the magnetic field to suppress the seed island. This means that the growth of the perturbed magnetic field is restricted by some mechanisms when the magnetic island disappears. This result means that some kinds of spontaneous current layer inside the plasma produce the perturbed magnetic field that suppresses the seed island in the LHD.

6. Summary

We applied the toroidal magnetic flux loop array in LHD to diagnose the magnetic island with $m/n = 1/1$ mode structure. The external perturbation coils impose a static resonant field with the $m/n = 1/1$ mode which resonates to the confinement magnetic field at the $\iota/2\pi = 1$ surface and produces the seed island with the $m/n = 1/1$ structure. When the magnetic island structure changes during a discharge, a perturbed magnetic field component originating from the plasma current appears and the flux loop array equipped in the LHD detects the toroidal profile of δb_1. The toroidal profile of δb_1 is decomposed into the $n = 1$ mode with the Fourier decomposition to obtain the $\delta b_1^{n=1}$ and the $\phi_{n=1}$. These parameters can define the structure of the magnetic island. The island width can be quantified with the magnetic diagnostics because the δb is proportional to the square root of the w as shown in Eq. (1). A non-zero $\delta b_1^{n=1}$ can be observed even when the magnetic island cannot be measured with the Thomson scattering system. The elucidation of the mechanism of the self-healing may lead to an explanation of the fundamental stabilization of the MHD mode caused by the magnetic island. Further study is intended to reveal the formation mechanism of the current layer producing the δb which affects the behavior of the magnetic island.

Acknowledgement

This study was supported by a Grant-in-Aid for Scientific Research (A) (No.17206094) from the Ministry of Education, Culture, Sports, Science and Technology of Japan. This work was supported by NIFS under Contract No.NIFS06ULHH518.

[1] T. Ozeki and JT-60 team, Plasma Phys. Control. Fusion **45**, 645 (2003).
[2] T.C. Hender *et al.*, Nucl. Fusion **44**, 788 (2004).
[3] K. Narihara *et al.*, Phys. Rev. Lett. **87**, 135002 (2001).
[4] N. Ohyabu *et al.*, Phys. Rev. Lett. **88**, 055005 (2002).
[5] N. Ohyabu *et al.*, Plasma Phys. Control. Fusion **47**, 1431 (2005).
[6] K. Narihara *et al.*, Rev. Sci. Instrum. **72**, 1122 (2001).
[7] A.H. Boozer, Phys. Fluids **27**, 2055 (1984).
[8] T. Morisaki *et al.*, Fus. Eng. Des. **65**, 475 (2003).
[9] Y. Narushima *et al.*, Proc. 31st EPS Conf. ECA Vol.28G, P-5.113 (2004).
[10] C.C. Hegna and A. Bhattacharjee, Phys. Fluids **B1**, 392 (1989).